I&EC research
Industrial & Engineering Chemistry Research
pubs.acs.org/IECR
Article

Energy and Economic Analysis of the Hydrothermal Reduction of CO_2 into Formate

Laura Quintana-Gómez, Lidia Martínez, Daniel Román-González, José Juan Segovia, Ángel Martín, and Maria Dolores Bermejo*

Cite This: *Ind. Eng. Chem. Res.* 2021, 60, 14038−14050

Read Online

ACCESS | Metrics & More | Article Recommendations | Supporting Information

ABSTRACT: In this work, the mass and energy balances and the economic analysis of a continuous process for the reduction of CO_2 (captured as $NaHCO_3$) into sodium formate using Zn as the reductant are studied. The reaction in hydrothermal media has the advantage of easily integrating the conversion system with the CO_2 capture process by absorption in basic solutions. The process conditions (pressure, $Zn/NaHCO_3$ molar ratio, and residence time) were theoretically optimized. A reaction temperature of 275 °C was selected, obtaining formate yields greater than 70%. A continuous process design was proposed based on available information and on our experimental experience in the process. Mass and energy balances were solved and the potential for an energy integration was studied. Additionally, both capital and operating costs for a plant treating 1000 kg/h of CO_2 were estimated. The cost calculated for transforming CO_2 was EUR 1.28/kg CO_2.

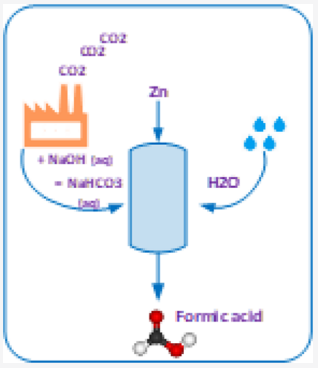

1. INTRODUCTION

A major consequence of the combustion of fossil fuels is the continuous and significant increase in atmospheric concentration of CO_2, a greenhouse gas. In the past decades CO_2 has gained great attention as a potential raw material due to its abundance, lack of toxicity, and relatively low price,[1] rather than considering it as just a waste substance. However, CO_2 industrial applications as a C1 building block are currently still limited to a few applications, such as the synthesis of urea and its derivatives, the production of salicylic acid and organic carbonates, the Solvay process for the synthesis of $NaHCO_3$−Na_2CO_3, and the synthesis of methanol using syngas enriched with CO_2.[2,3]

Different methods have been proposed for reducing CO_2 into useful chemicals and fuels, such as hydrogenation of CO_2 and electrochemical or photochemical conversion, among others. Nevertheless, due to their low yields and high cost, these technologies still need further development.[4] Moreover, although the catalytic hydrogenation of CO_2 is one of the most popular alternatives,[5] it requires the addition of gaseous H_2. Currently, H_2 is mainly produced from fossil fuels using energy-intensive processes, such as steam methane reforming.[6] Although in the past years, great efforts have been made to produce green hydrogen by water electrolysis and electric energy from renewable sources, this technology is still not economically competitive in comparison to steam methane reforming.[7] The high costs associated with these processes, along with the unfavorable flammability and compressibility of H_2,[8] have triggered interest in investigating the feasibility of other options, such as in situ H_2 generation by using water as the reaction media and hydrogen donor. Indeed, among other advantages, high-temperature water (HTW) is regarded as an environmentally friendly solvent.[9]

Nowadays, CO_2 capture is mainly based on its absorption on aqueous basic solutions of amines or NaOH. Although this is a well-known technology, the high costs associated with CO_2 desorption, purification, compression, and storage have limited its industrial application.[10,11] The economic cost of CO_2 from concentrated sources, such as the cement industry, can be found in the literature. Using NaOH as absorbent, Proaño et al.[12] estimated a cost of USD 59/ton CO_2 based on operating costs.

Direct reduction of CO_2 dissolved in aqueous solutions would represent a huge advantage and would permit developing integrated systems for CO_2 capture and utilization. Such direct CO_2 reduction would allow avoiding the costly CO_2 purification and compression steps. In the past years, investigations on the hydrothermal reduction of CO_2 have developed rapidly, and different products such as formic acid,[13,14] methanol,[15,16] and methane[17,18] have been synthesized. Among them, formic acid has attracted great interest due to its widespread use in the agricultural, leather, and dye industries. Formic acid is also regarded as a potential hydrogen

Received: May 25, 2021
Published: September 22, 2021

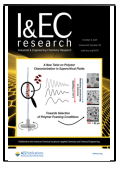

https://doi.org/10.1021/acs.iecr.1c01961
Ind. Eng. Chem. Res. 2021, 60, 14038−14050

storage vector.[13] Fe, Al, Zn, and Mn have been proposed as reducing agents in the hydrothermal reduction of CO_2 into formic acid, methane, methanol, or phenol,[14,17,19−23] alone or combined with catalysts such as Ni or Cu.[16,18,24] Alternatively, alcohols including biomass derivatives can also be used as reductants in hydrothermal CO_2 reactions.[9,13,25] The reduction of CO_2 using biomass derivatives in a continuous plant is a well-known technology in our research group, where a continuous pilot plant was designed for the reaction of a concentrated solution of $NaHCO_3$ and glucose. It is worth noting that the reaction temperature of 300 °C and a pressure of 200 bar is kept through the reactor.[26]

To the best of the authors' knowledge (with the exception of the work of Takahashi et al.,[5] who reported the hydrothermal reduction of CO_2 in a semicontinuous system), this is the first approach to develop a continuous process for hydrothermal CO_2 conversion. The main objective of this study was to investigate the feasibility of converting CO_2 absorbed as $NaHCO_3$ into sodium formate (HCOONa) in a continuous process using Zn as the reductant. It is worth mentioning that Zn is capable of reducing CO_2 at higher yields and in shorter times than other metals without the addition of a catalyst.[22] For this reason, our team decided to study the design of this process based on the development of the basic engineering according to the mass and energy balances. The project provided an exciting opportunity to advance our knowledge of the development of continuous processes for CO_2 utilization combined with CO_2 capture. To conduct the energy and economic analysis of the continuous hydrothermal reduction of CO_2 into formate, the first step was to summarize the main aspects of the hydrothermal CO_2 conversion based on a previous study by our research group.[21] Afterward, a flow diagram for the process was proposed, describing the main units. Next, two different alternatives for the reactor type were suggested. Finally, mass and energy balances, along with an economic evaluation of the process, were conducted.

2. DESIGN BACKGROUND

In a previous study by this research group, hydrothermal CO_2 conversion (captured as $NaHCO_3$) was investigated in bench-scale batch reactors with a volume of 15 mL made of tubing. Roman-Gonzalez et al.[21] reported conversions up to 60% and a selectivity to sodium formate of nearly 100% operating in batch mode. This made the process described an attractive candidate to be studied as a continuous process. Roman-Gonzalez et al.[21] proposed a mathematical model of the batch reactor capable of predicting the formate formation yields with an averaged deviation of 3.5% based on reactions R1 to R5.

$$HCO_3^-(aq) + Zn(s) \rightarrow HCOO^-(aq) + ZnO(s) \quad (R1)$$

$$H_2O(l) + Zn(s) \rightarrow H_2(aq) + ZnO(s) \quad (R2)$$

$$HCO_3^-(aq) + H_2(aq) \rightarrow HCOO^-(aq) + H_2O(l) \quad (R3)$$

$$HCOO^-(aq) + H_2O(l) \rightarrow HCO_3^-(aq) + H_2(g) \quad (R4)$$

$$HCOO^-(aq) \rightarrow CO(g) + OH^-(aq) \quad (R5)$$

These reactions can be divided in two groups. Reactions R1 and R2 are characterized by a high reaction rate, and they are responsible for oxidizing Zn into ZnO. Reaction R3 dominates the second step, and the remaining HCO_3^- is converted into $HCOO^-$. At long reaction times (≥120 min), particularly at $T \geq 300$ °C, formic acid yield slightly decreases due to reactions R4 and R5.[21,22] It should be remarked that in the model, the effect of reaction R5 was considered negligible because the contribution of reaction R5 to formate decomposition is very small in comparison to that of reaction R4.[21] It is worth mentioning that reactions R3 and R4 are the direct and reverse reactions of an equilibrium reaction. However, in the model they were expressed as independent reactions to facilitate the nomination of the kinetic constants.[21]

To represent the process, for the reactions in which Zn was involved, the shrinking core model was chosen, assuming that reaction kinetics was the controlling step. Reaction rates were thus proportional to the surface area of the solid in reactions involving Zn. This area depended on the number of particles in the reactor (n_p) and on the unreacted core radius of particles (r). The solid particles were considered as spheres; the reaction rates for reactions R1−R5 are therefore expressed in eq 1−5:[21]

$$r_1 = 4\pi r^2 n_p k_1 C_{HCO_3^-} \quad (1)$$

$$r_2 = 4\pi r^2 n_p k_2 \quad (2)$$

$$r_3 = k_3 C_{HCO_3^-} C_{H_2} \quad (3)$$

$$r_4 = k_4 C_{HCOO^-}^n \quad (4)$$

where n is the exponent in the kinetic equation and it is given by eq 5:[21]

$$n = 1.4671 + \frac{25.6595}{T} + 0.0007024 \ln T \quad (5)$$

and T is expressed in K.

Roman-Gonzalez et al.[21] described the influence of different reaction parameters such as temperature, $Zn/NaHCO_3$ ratio, and pressure, reporting the highest formate yields at 275 °C. They also described the importance of the heating rate and concluded that formate yield increased for higher heating rates, which promote the rate of reaction 1. In agreement with Jin et al.,[22] Roman-Gonzalez et al.[21] suggested that high $Zn/NaHCO_3$ ratios also favored the progress of reaction 1, increasing formate yield and thus producing more H_2, which increases H_2 solubility in water. The same effect can be achieved using higher pressures to promote H_2 solubility in the aqueous phase. This, in turn, enhances the rate of reaction 3, improving formate yield while keeping the $Zn/NaHCO_3$ ratio low.

It should be stressed that aqueous $NaHCO_3$ involves different ionic species, which may behave differently during reaction, as indicated in reactions R6−R9. Equations 6−9 describe the different equilibrium relations of all these species:[27]

$$CO_2(g) + H_2O \rightleftharpoons H_2CO_3(aq) \quad (R6)$$

$$K_0 = \frac{[H_2CO_3]}{P_{CO_2}} \quad (6)$$

where K_0 is the molar solubility expressed in mol/(L·atm), $[H_2CO_3]$ is the concentration of CO_2 dissolved in the water, and P_{CO2} is the partial pressure of CO_2.

$$H_2CO_3(aq) \rightleftharpoons HCO_3^-(aq) + H^+(aq) \quad (R7)$$

https://doi.org/10.1021/acs.iecr.1c01961
Ind. Eng. Chem. Res. 2021, 60, 14038−14050

$$K_1 = \frac{[HCO_3^-][H^+]}{[H_2CO_3]} \quad (7)$$

$$HCO_3^-(aq) \rightleftharpoons CO_3^{2-}(aq) + H^+(aq) \quad (R8)$$

$$K_2 = \frac{[CO_3^{2-}][H^+]}{[HCO_3^-]} \quad (8)$$

$$H_2O \rightleftharpoons H^+(aq) + OH^-(aq) \quad (R9)$$

$$K_W = [H^+][OH^-] \quad (9)$$

The value of the dissociation constants varies with the temperature.[27] According to Roman-Gonzalez et al.,[21] calculations of the reaction conditions indicated that most of the CO_2 dissolved in the aqueous medium at hydrothermal reaction conditions was in the form of HCO_3^-. Indeed, Roman-Gonzalez et al.[21] concluded that the carbonic acid/bicarbonate equilibrium was displaced toward bicarbonate, especially at long reaction times. Moreover, despite a decrease in the calculated pH during reaction time, it remains alkaline (pH > 10). It is important to highlight that the formation of CO via reverse water gas shift (RWGS) reaction is avoided due to the high H_2O/CO_2 ratio.

3. PROCESS DESCRIPTION

On the basis of these previous results, a continuous process for hydrothermal conversion of CO_2 into formate has been proposed. The initial conditions of this process are summarized in Table 1. It was considered that CO_2 was already captured as an aqueous solution of $NaHCO_3$ with a concentration of 1.2 M. The amount of CO_2 treated was 1000 kg/h, which corresponded to about 20800 kg/h of aqueous $NaHCO_3$. Zn was used as the reductant. The initial $NaHCO_3$ concentration was selected based on the saturation concentration of $NaHCO_3$ in water at room temperature. The higher is the concentration, the smaller is the size of the equipment; this, in turn, reduces capital costs. Moreover, higher concentrations reduce the amount of water needed for a given quantity of captured CO_2, so pumping and heating costs also decrease. Yoo et al.[28] studied the capacity of sodium hydroxide aqueous solutions to capture CO_2 in the form of $NaHCO_3$ in a batch reactor. Depending on the amount of NaOH present in the aqueous solution and on the reaction time, they reported values of $NaHCO_3$ formation that ranged from 0.23 M after 20 min with a 1 wt % of NaOH to approximately 1.14 M with a 5 wt % of NaOH.[28] Although this process was proposed based on the results of previous work by this research group,[21] it should be noted that the mixing and homogenization characteristics of the solids and liquid in the reactor have not been experimentally studied and they should be investigated in the future. Figure 1 shows the proposed flow diagram of the process.

Table 1. Initial Conditions of the Proposed Continuous Process for the Conversion of CO_2 into Formate

parameter	value
CO_2 treated	1000 kg/h
$NaHCO_3$ mass flow rate	20800 kg/h
$NaHCO_3$ concentration	1.2 M
initial pressure (P)	1 bar
initial temperature (T)	25 °C

The main steps of the hydrothermal process presented in Figure 1 are as follows:

(1) The CO_2 absorbed as a solution of $NaHCO_3$ with a concentration of 1.2 M at room conditions (Stream 1) is pressurized in the pump (P-1) up to the operating pressure (Stream 2).
(2) In the heat exchanger E-1, Stream 2 is heated to a temperature high enough (Stream 3) to be able to heat the solid Zn (Stream 4) by direct contact from room temperature in such a way that the mixed solutions + the solid Zn are at the operating temperature.
(3) The solution is mixed with the solid Zn particles stored in a hopper. In the simulations performed in a previous study,[21] it was found that heating the Zn rapidly was essential for achieving a good yield in the process. If Zn were heated beforehand, the hydrogen would release and formate would be produced by the slow reaction of gaseous H_2 with bicarbonate (reaction R3) instead of the rapid direct reaction with Zn (reaction R1). To achieve that, Zn will be directly injected into the bicarbonate solution using a hopper. It is worth mentioning that the feed hopper of the Zn (TK-1) is pressurized at the operating pressure under N_2 to avoid oxidation of Zn particles. The mixture of the $NaHCO_3$ solution with Zn takes place through a three-way valve (V-1), producing Stream 5, which is fed into the reactor.
(4) In the reactor (R-1), aqueous $NaHCO_3$ is reduced into formate according to reactions R1 and R3. Stream 6 contains the products and the unreacted reactants along with the Zn in the form of ZnO. As stated in reactions R1 and R2, Zn is oxidized very rapidly.[21,22]
(5) The hydrocyclone (S-1) is where the ZnO is separated from the fluid. As a result, Stream 6 is divided into Stream 7 (solids) and Stream 8 (the liquid and gas products along with unreacted $NaHCO_3$).
(6) To save energy, Stream 8 is used to preheat the feed in the heat exchanger E-1 as the hot stream, reducing its own temperature.
(7) As additional cooling is still needed, Stream 9 leaves the heat exchanger and passes through the cooler C-1, where it is cooled down to 35 °C.
(8) Stream 10 is depressurized through an isenthalpic valve.
(9) Stream 11, which is already at atmospheric pressure, is separated into its gaseous and liquid components in the flash chamber (S-2). Therefore, Stream 12 contains the gas products, while Stream 13 consists of the sodium formate, the unreacted bicarbonate, and the gases dissolved in the aqueous solution.

4. PROCESS DEVELOPMENT

4.1. Reactor Model. The continuous plug flow reactor was modeled considering the concentration profiles obtained using eqs 10−13, where τ is the residence time of the liquid phase in the plug flow reactor. In the case of the hydrogen balance, the pressure in the plug is fixed and controlled by a back-pressure valve, and this pressure in turn determines maximum hydrogen solubility in the liquid phase at the operating temperature. When the amount of produced hydrogen exceeds its solubility, the excess amount of gas is transferred to the gaseous phase. Therefore, in the model, hydrogen concentration is calculated

https://doi.org/10.1021/acs.iecr.1c01961
Ind. Eng. Chem. Res. 2021, 60, 14038−14050

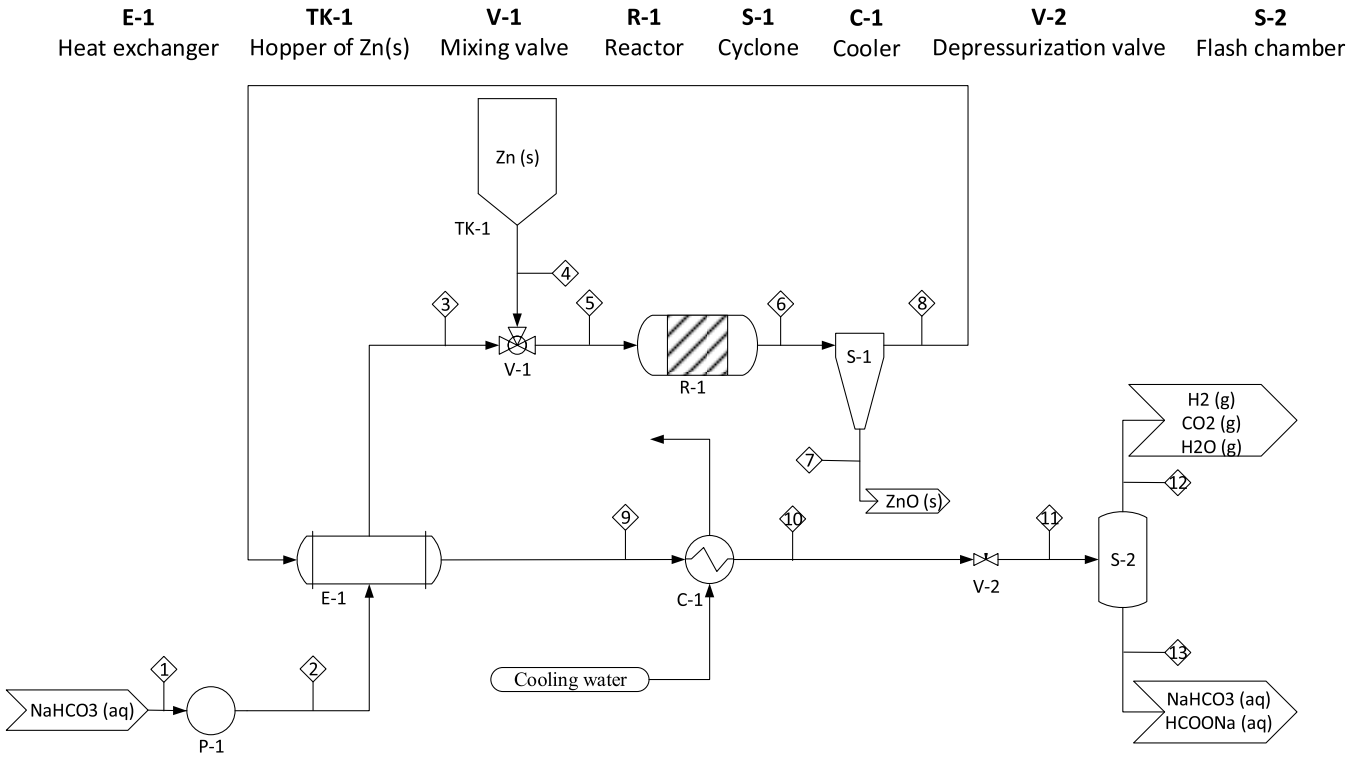

Figure 1. Flow diagram of a continuous plant for hydrothermal CO_2 conversion.

as the minimum between the concentration calculated with the mass balance and the solubility concentration.

$$\frac{\partial c_{HCO_3^-}}{\partial \tau} = -r_1 - r_3 + r_4 \tag{10}$$

$$\frac{\partial c_{HCOO^-}}{\partial \tau} = r_1 + r_3 - r_4 \tag{11}$$

$$\frac{\partial c_{H_2}^{\text{BALANCE}}}{\partial \tau} = r_2 - r_3 + r_4 \tag{12}$$

$$c_{H_2} = \min(c_{H_2}^{\text{BALANCE}}, c_{H_2}^{\text{SOLUBILITY}}) \tag{13}$$

As an alternative to a plug flow reactor, a continuous stirred-tank reactor (CSTR) was also simulated. The presence of solid particles can be an operating challenge that could be minimized using a CSTR.

The CSTR simulation considered that the residence time was much higher than the time that Zn needs to react, and that the Zn particle radius was zero. Therefore, reactions R1 and R2 were not considered. Other assumptions made were that the $Zn/NaHCO_3$ mole ratio was 1 and that the H_2 concentration in the liquid was its solubility at the reaction temperature and pressure. All these considerations lead to eq 14 and 15, to calculate CSTR concentration of HCO_3^- and $HCOO^-$, respectively.

$$C_{HCO_3^-} = C_0 - \tau(r_3 - r_4) \tag{14}$$

$$C_{HCOO^-} = \tau(r_3 - r_4) \tag{15}$$

where τ is the residence time and r_3 and r_4 are the reaction rates of reactions R3 and R4 calculated according to eq 3 and 4, respectively.

4.2. Mass and Energy Balances. *Mass Balances.* To calculate the mass balances, the first step is to know the $Zn/NaHCO_3$ optimal ratio, which makes it possible to calculate the amount of Zn necessary to conduct the reactions. The conversion of $NaHCO_3$ achieved and the yield to the different products are crucial for determining the composition of the product stream. The yield to products was calculated according to eq 16.

$$Y_i = \frac{\text{mole of } i \text{ obtained}}{\text{theoretical mole of } i} 100 \tag{16}$$

It is important to highlight that to calculate the mass balances, $NaHCO_3$ is considered as a single component during the entire process. However, when the flash chamber is reached (Figure 1), it is considered that the $NaHCO_3$ is decomposed in its equilibrium species according to the equilibrium reactions R6–R9 to calculate the amount of CO_2, which is separated in the flash chamber. The concentration of each species was calculated with Matlab, using the program *BicarbonateEquilibrium* shown in the Supporting Information. Briefly, the main feature was the implementation of eq 6–9 to establish the relations between all the equilibrium species formed from aqueous $NaHCO_3$ as a function of the temperature. The code programmed in Matlab makes it possible to calculate the number of moles of CO_2 present in the mixture.

Matlab was also used to calculate the amount of the components separated in each phase in the flash chamber. The code defined for these calculations, called *PSRKtricomponent*, is detailed in the Supporting Information.

Energy Balances. The enthalpy of each stream was calculated as the sum of the enthalpies of all its components (eq 17). In the case of the aqueous streams containing $NaHCO_3$, Na_2CO_3, NaOH, H_2CO_3, and HCOONa, the enthalpy of the stream was considered as the enthalpy of the

https://doi.org/10.1021/acs.iecr.1c01961
Ind. Eng. Chem. Res. 2021, 60, 14038−14050

pure water, because the enthalpy of the solid compound can be assumed as negligible in comparison to that of water.

$$\Delta H = \sum_{i=1}^{n} \Delta H_i \tag{17}$$

$$\Delta H = m_i \int_{T_{ref}}^{T} C_p \, dT \tag{18}$$

It is important to highlight that the assumed reference state was 25 °C and 1 bar. The enthalpies of Zn and ZnO were calculated using eq 18. The expressions for C_p used are gathered in Table S1 (Supporting Information).[29] The thermodynamic properties of the water were calculated using Water97_v13.xla, which is an Add-In for MS Excel that calculates the properties of the water based on the industrial standard IAPWS-IF97.[30] CO_2 and H_2 enthalpies were calculated with the NIST Chemistry WebBook: Thermophysical Properties of Fluid Systems.[31] The process was assumed to be adiabatic, and momentum balance was not taken into consideration.

To calculate the energy balance in the reaction step, eq 19 was used. This equation allows calculation of the temperature of the stream leaving the reactor. The values of the enthalpy of formation for the species involved in the production of HCOONa are gathered in Table S2 (Supporting Information).[29,32]

$$\sum (\Delta H_{f,\text{reactants}} + \Delta H_{\text{reactants}}) = \sum (\Delta H_{f,\text{products}} + \Delta H_{\text{products}}) \tag{19}$$

where ΔH_f is the enthalpy of formation of each compound.

4.3. Economic Evaluation. *Capital Costs.* The total physical capital costs of the process were estimated using eq 20, based on the Lang factors.[33]

$$\text{PPC} = \text{PCE}(1 + f_1 + f_2 + \ldots + f_9) \tag{20}$$

where PPC is the total physical plant cost, PCE is the total cost of the main pieces of plant equipment and the Lang factors f_1, f_2, etc. for a mixed fluids−solids processing can be found in the reference material.[33] The fixed capital costs were calculated using eq 21.[33] The Lang factors f_{10} to f_{12} can also be found in the reference material.[33]

$$\text{fixed capital} = \text{PPC}(1 + f_{10} + f_{11} + f_{12}) \tag{21}$$

The capital cost for the heat exchanger, the cooler, and the hopper, as well as that of the boiler, which is needed to start plant operation, were calculated using eq 22.[34] It is worth mentioning that the heat exchanger selected is a tube and shell and that the cost of the hopper, as it is under high pressure, is estimated as the cost of a pressurized vessel.

$$C_e = a + bS^n \tag{22}$$

where C_e is the cost of the equipment in USD (January 2010, CEPCI = 532.9); a and b are constants detailed in Table S3 in the Supporting Information; S is the size of each unit, that is, the area of the heat exchanger and cooler and the mass of the hopper, with the units detailed in Table S3 in the Supporting Information; and n is an exponent based on the type of equipment, also specified in Table S3.[34]

The cost of the pump was estimated with eq 23:[35]

$$\text{pump cost} = \left(\frac{P}{74.6}\right)^{0.67} \times 4400 \tag{23}$$

where the cost is in USD (1968, CEPCI = 113.6) and P is the power required in kW.

To update the historical cost data, eq 24 was used to relate present cost to past cost.[34] The average Chemical Engineering Plant Cost Index (CEPCI) in 2019 was 607.5.[36]

$$\text{cost in year } A = \text{cost in year } B \frac{\text{cost index in year } A}{\text{cost index in year } B} \tag{24}$$

To calculate the cost of each piece of equipment, its capacity must be calculated. The power of the pump was taken from Aspen One v.10 simulation software. To estimate this value, an efficiency of 0.6 for the pump and 0.9 for the driver was assumed. The area of the heat exchanger and the cooler can be calculated according to eq 25:[35]

$$A_{\text{heat exchanger}} = \frac{Q_{\text{heat-duty}}}{U \times \Delta T_{\text{lm}}} \tag{25}$$

where A is the area of the heat exchanger in m^2, $Q_{\text{heat-duty}}$ is the energy required for heating or cooling in kW, U is the overall heat transfer coefficient in kW/m^2 K, and ΔT_{lm} is the logarithmic mean temperature difference in K. The value of the coefficient U for a shell and tube heat exchanger with liquid water in both sides was estimated at 1300 W/m^2 K.[37]

The reactor proposed in this case was a tubular plug flow reactor. To choose the correct material for constructing the reactor, you must take not only high pressure and temperature conditions into account, but also the in situ H_2 formation and the negative effects that this may cause in the reactor walls. Introducing hydrogen into a metallic material can cause degradation of its mechanical properties, a phenomenon known as hydrogen embrittlement (HE) or hydrogen-assisted cracking (HAC), since the hydrogen is not the only contributor to this problem.[38] However, austenitic stainless steels, particularly Type 316 and 316 L, are more stable than other metallic materials, and their use is recommended in the presence of high pressure hydrogen.[39] As for hydride formation as the main cause for HAC, it is important to highlight that Groups IV and V metals and their alloys show the strongest tendency toward hydride formation; however, steels (including supermartensitic stainless steel [SMSS]) are known to be nonhydride forming materials.[40]

For cost estimation, a 316 stainless steel pipe was selected. Because the reactor works at high pressure, reactor cost is obtained by multiplying its mass by the price of the stainless steel in EUR per ton. The price of stainless steel 316 bar in Europe is EUR 3181/ton.[41] Pipe length is a function of the diameter and volume, as it is considered as a cylinder and calculated with eq 26. Given that the reactor is considered as a stainless steel pipe, pipe volume can be calculated using eq 27 (the standard equation for calculating reactor volume), multiplying the volumetric flow rate by the residence time.

$$L = \frac{V4}{\pi D^2} \tag{26}$$

where

$$V = \tau \vartheta \tag{27}$$

where τ is the residence time and ϑ is the volumetric flow rate.

https://doi.org/10.1021/acs.iecr.1c01961
Ind. Eng. Chem. Res. 2021, 60, 14038−14050

As mentioned earlier, H_2 is also present in the reactor. Therefore, it is necessary to determine the liquid holdup in the two-phase flow to determine reactor volume. The volume calculated with eq 27 needs to be multiplied by the liquid holdup. This factor is obtained using the Lockhart−Martinelli parameter X, calculated with eq 28.[42]

$$X = \left[\frac{V_g \rho_g \mu_l}{V_l \rho_l \mu_g}\right]^m \frac{\rho_l V_l^2}{\rho_g V_g^2} \tag{28}$$

where $m = 0.2$ is the value for turbulent flow in this case; V is the velocity (m/s), in this case $V_l = 0.079$ m/s and $V_g = 0.013$ m/s; μ is the viscosity (Pa·s); and ρ is the density (kg/m^3). The subscripts g and l refer to the gas and liquid phases, respectively.

Pipe thickness was calculated with the ASME standard B31.3, which defines the minimum pipe thickness (eq 29) as the sum of the pressure design thickness (t) and the corrosion allowance (c), taken as 0.125 in.

$$t_m = t + c \tag{29}$$

where t is calculated according to eq 30

$$t = \frac{PD}{2(SE + PY)} \tag{30}$$

where t is the pressure design thickness (in); P is the internal design pressure gauge (psig); D is the outside diameter of the pipe; S is the stress value of the stainless steel (approximately 13000 psi); E is the weld joint quality factor, which for a seamless pipe is 1; and Y is the temperature coefficient (0.4 in this case).

Once the reactor thickness and length are known, its mass can be calculated taking into account that the density of stainless steel is 8.03 g/cm^3.

The cost of the cyclone was estimated using Matches equipment cost estimator.[43] The cost of the hopper was estimated as a vertical pressurized vessel according to eq 22, taking into account that the deposit is filled with Zn every day. For estimating the capacity of the flash, it was assumed that the residence time in the flash was 2 min. As the flash is at room conditions, it is considered as a stainless steel tube with an outside diameter of 8 in.

Operating Costs. In addition to the fixed capital costs, the operating costs also need to be estimated. The operating costs are divided in turn into two groups: (i) fixed operating costs, which are independent from the production rate, and (ii) variable operating costs, such as the cost of raw materials and utilities, that vary with the amount of product synthesized.[33] In this project, the operating costs are estimated on an annual basis.

The bicarbonate is not considered as a cost, as it is generated in a process of CO_2 capture. However, the NaOH necessary to capture the CO_2 is recorded as a cost. The price of Zn is EUR 1997/ton[44] and the price of NaOH is EUR 320/ton.[45] Moreover, N_2 is necessary to pressurize the hopper; this N_2 is generated using a N_2 generator with pressure swing adsorption (PSA) technology. The cost for small flow N_2 generators generally varies between EUR 2500 and EUR 18000. In this case, a cost of EUR 18000[46] was assumed. The updated operating cost of the N_2 generator can be taken to be EUR 1.6/m^3 N_2.[47] The utilities considered are the process water and also the power needed to operate the plant (specifically, the electricity needed by the pump and to regenerate the ZnO). The price of water varies significantly depending on the location. For a plant located in the Valladolid area (Spain), the overall price of industrial water would be approximately EUR 1.9/m^3.[48] In Spain the cost of industrial electricity is on average EUR 0.075/kWh.[49]

The regeneration of waste materials, particularly ZnO, also needs to be considered. Nowadays, Zn is usually recovered from oxide by electrolysis with sulfuric acid following reactions R10 and R11. During electrolysis, O_2 is formed from water at the positive electrode while Zn is deposited on the negative electrode. The sulfuric acid is held at temperatures from 35 to 38 °C. The positive electrode is made from Pb−Ag alloys, and the process consumes between 3.25 and 3.80 kWh/kg Zn.[50] In this study, a consumption of 3.25 kWh/kg Zn was assumed. The cost of sulfuric acid is EUR 47/ton.[51]

$$ZnO + H_2SO_4 \rightarrow ZnSO_4 + H_2O \tag{R10}$$

$$2ZnSO_4 + 2H_2O \rightarrow 2Zn + 2H_2SO_4 + O_2 \tag{R11}$$

As for the operating labor, it can be considered that there are three workers per shift. Taking into account that this process would run continuously, five shifts were assumed. In 2019, the cost per worker in the industrial sector in Spain was EUR 37822.88 annually.[52]

The fixed operating costs include plant maintenance, insurance, and taxes, among others. The annual maintenance costs for chemical plants range from 5% to 15% of the installed capital costs. In this case, it was assumed that the maintenance cost is 5%. There are also other plant supplies such as safety clothing, cleaning materials, etc. that can be estimated as 10% of the total maintenance cost.[33] Other variable costs include supervision and management (taken as 25% of the operating labor[34]); general plant costs such as plant security and clerical staff, among others, assumed to be 50% of the labor costs; a depreciation allowance, taken as 10% of the fixed capital; and local taxes, insurance, and royalties, each one considered as 1% of the fixed capital.[33]

5. RESULTS AND DISCUSSION

5.1. Process Optimization. The kinetic constants obtained in previous work by this research group[21] were used to develop a model of the continuous reactor based on reactions R1−R4. This model was used to optimize the reaction conditions that enhance the yield of HCOONa produced.[21] The parameters evaluated included the Zn/$NaHCO_3$ molar ratio and pressure in the reactor. The initial concentration of $NaHCO_3$ solution to start the simulation was equal to 1.2 M. According to the experimental results reported by Roman-Gonzalez et al.,[21] the temperature was fixed at 275 °C to minimize formate decomposition. The optimal conditions obtained in the model of the continuous reactor were applied to the process design.

Higher Zn/$NaHCO_3$ ratios and higher pressures improved the formate yields by enhancing the rates of reactions R1 and R3.[21] However, when designing a process, it is crucial to keep in mind that excess Zn not only increases the costs of the process but also generates more waste of ZnO that should be regenerated. The yield can be raised instead by increasing the pressure and, thus, H_2 solubility. Increasing the pressure will increase the purchase cost of the reactor because the wall is thicker. However, this alternative is cheaper than using a large amount of Zn.

https://doi.org/10.1021/acs.iecr.1c01961
Ind. Eng. Chem. Res. 2021, 60, 14038−14050

Figure 2 shows the changes in sodium formate yield as a function of pressure after a three-hour reaction in a continuous

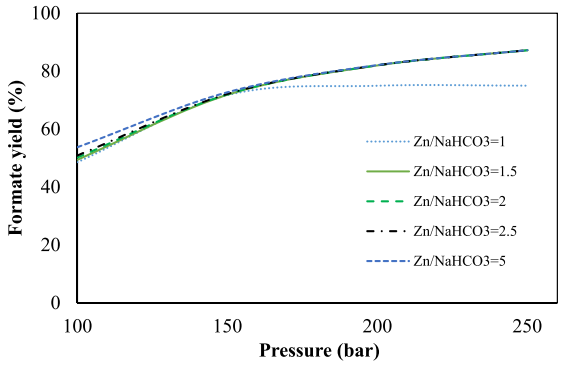

Figure 2. Sodium formate production and pressure achieved based on the simulation model for a continuous plug flow reactor for different $Zn/NaHCO_3$ mole ratios at 275 °C. Initial $NaHCO_3$ concentration was 1.2 M, and reaction time was 3 h.

plug flow reactor using different $Zn/NaHCO_3$ mole ratios. It can be seen that the main influence stems from the pressure being independent of the excess Zn. Consequently, working with a low $Zn/NaHCO_3$ mole ratio was selected. Figure 2 shows that for pressures higher than 200 bar there are no significant changes in the formate yield, so this pressure was selected as the optimum. At 200 bar, with the exception of $Zn/NaHCO_3$ mole ratio of 1, the remaining ratios evaluated gave similar yields. Therefore, a $Zn/NaHCO_3$ mole ratio of 1.5 was selected. Under these conditions the sodium formate yield reached 82%.

In a continuous flow reactor, the formate yield varies with residence time for different $Zn/NaHCO_3$ mole ratios, as plotted in Figure 3. The initial concentration of $NaHCO_3$

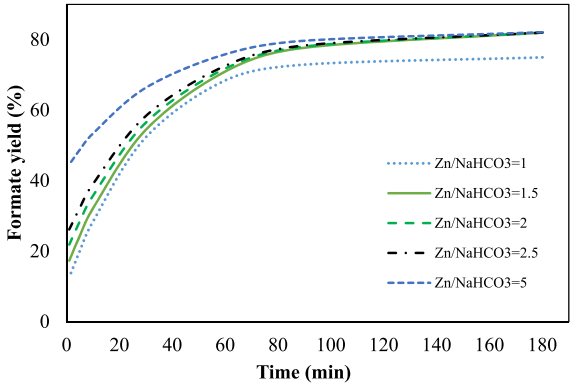

Figure 3. Evolution of the sodium formate yield with the residence time in a continuous plug flow reactor at different $Zn/NaHCO_3$ mole ratios; T = 275 °C, P = 200 bar, and initial $NaHCO_3$ concentration of 1.2 M.

considered was 1.2 M, with a pressure of 200 bar. Figure 3 clearly reveals that at short reaction times, the effect of $Zn/NaHCO_3$ mole ratio has an important influence on formate yield. For a ratio of 5, after 1 min of reaction the yield reached 45%. For reaction times higher than 60 min, the effect of the $Zn/NaHCO_3$ mole ratio is almost insignificant. In the case of the selected $Zn/NaHCO_3$ mole ratio of 1.5, the yield was 24% for a residence time of 5 min, while at 30 min it rose to 55%. Between 60 and 180 min, the formate yield increased by only 11%. Therefore, the residence time was set to 60 min, when the yield was 71%. It is worth mentioning that considering shorter times as the optimum ones would strongly reduce reactor size and, in turn, its costs.

As mentioned before, a CSTR was also simulated because it would facilitate handling solids in the reactor. Figure 4 shows

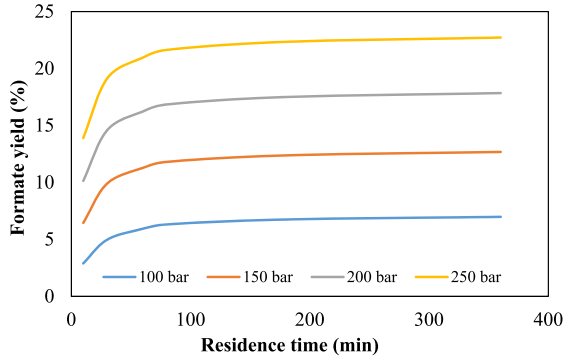

Figure 4. Evolution of the sodium formate yield with the residence time in a CSTR at different pressures. $Zn/NaHCO_3$ = 1; T = 275 °C and initial $NaHCO_3$ concentration = 1.2 M.

the variation of the formate yield with the residence time at different pressures in a CSTR. It is clear from Figure 4 that the yields achieved were much lower than in the case of a plug flow reactor (Figure 3). Likewise, in the case of the simulation in a tubular reactor shown in Figure 3, the yield remained almost constant for residence times higher than 60 min, due to the fact that the equilibrium between reactions R3 and R4 is established at that time. As expected, higher yields were obtained at higher pressures. In a CSTR at 250 bar, the yield obtained for a residence time of 80 min was 22%, more than three times lower than in a tubular reactor at 60 min. Despite the advantage of easier manipulation of solid Zn in the CSTR, the option of the tubular reactor was chosen, along with a $Zn/NaHCO_3$ ratio = 1.5, P = 200 bar, and a residence time = 60 min, to obtain a formate yield of 71%.

The optimal reaction conditions and the yields of the products obtained under the optimal conditions calculated according to eq 16 are shown in Table 2.

Table 2. Optimal Reaction Conditions for the Hydrothermal Conversion of $NaHCO_3$ into Sodium Formate and Yields Obtained at Those Conditions

reaction conditions	optimum
$Zn/NaHCO_3$ mole ratio	1.5
pressure	200 bar
temperature	275 °C
residence time	60 min
reactor type	continuous plug flow reactor
Y_{HCOONa}	71%
Y_{ZnO}	100%
Y_{H_2}	52.7%

5.2. Hydrothermal Conversion of $NaHCO_3$ into Formate. Table 3 shows the main characteristics of each stream, including the pressure, temperature, and mass and energy balances. The name of the compounds in Table 3, along with their chemical formulas, are gathered in Table S4 in the Supporting Information. The optimal reaction temperature

https://doi.org/10.1021/acs.iecr.1c01961
Ind. Eng. Chem. Res. 2021, 60, 14038−14050

Table 3. Characterization of the Streams Involved in the Continuous Hydrothermal Conversion of $NaHCO_3$ into Formate, Including Their Mass and Energy Balances[a]

stream	1	2	3	4	5	6	7	8	9	10	11	12	13
P (bar)	1	200	200	200	200	200	200	200	200	200	1	1	1
T (°C)	25	25	277	25	275	301	301	301	45	35	39	39	39
substance(kg/h)													
$NaHCO_3$	1909	1909	1909	-	1909	554	21	533	533	533	455	-	455
Na_2CO_3	-	-	-	-	-	-	-	-	-	-	37	-	37
NaOH	-	-	-	-	-	-	-	-	-	-	0.03	-	0.03
H_2CO_3	-	-	-	-	-	-	-	-	-	-	0.6	-	0.6
CO_2	-	-	-	-	-	-	-	-	-	-	0.7	0.7	0.01
H_2O	18880	18880	18880	-	18880	18550	701	17850	17850	17850	17850	25	17830
Zn	-	-	-	2228	2228	-	-	-	-	-		-	-
HCOONa	-	-	-	-	-	1096	41	1055	1055	1055	1055	-	1055
ZnO	-	-	-	-	-	2775	2775	-	-	-	-	-	-
H_2	-	-	-	-	-	36	1.4	35	35	35	35	35	0.03
Total(kg/h)	20790	20790	20790	2228	23020	23020	3540	19480	19480	194780	19440	60	19380
H(kJ/h)													
$NaHCO_3$	0	0	0	0	0	0	0	0	0	0	0	-	0
Na_2CO_3	-	-	-	-	-	-	-	-	-	-	0	-	0
NaOH	-	-	-	-	-	-	-	-	-	-	0	-	0
H_2CO_3	-	-	-	-	-	-	-	-	-	-	0	-	0
CO_2	-	-	-	-	-	-	-	-	-	-	9	8	0.16
H_2O	0	345170	21025000		20800000	22950000	867100	22080000	1801600	1063700	1065400	1463	1064000
Zn	-	-	-	0	227900	-	-	-	-	-	-	-	-
HCOONa	-	-	-	-	-	0	0	0	0	0	0	0	0
ZnO	-	-	-	-	-	432300	432300	-	-	-	-	-	-
H_2	-	-	-	-	-	150350	5682	144700	26630	8682	6976	6971	5
H Total(kJ/h)	0	345170	2102500	0	21025000	23528000	1305100	22223000	1828200	1072400	1072400	8442	1064000

[a]A dash indicates that the compound is not present in the stream. Streams are numbered according to Figure 1.

https://doi.org/10.1021/acs.iecr.1c01961
Ind. Eng. Chem. Res. 2021, 60, 14038−14050

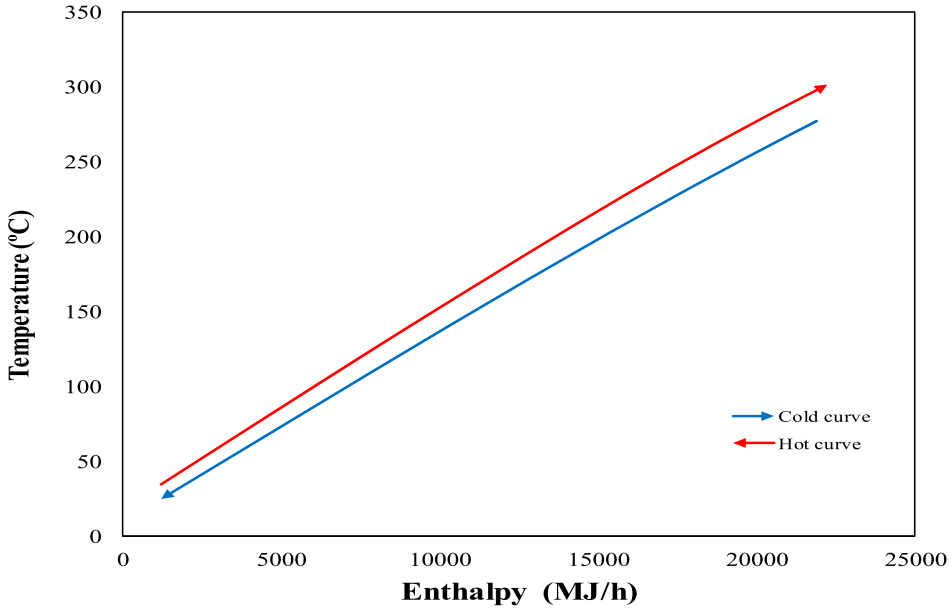

Figure 5. Heat integration curves.

is 275 °C; therefore, in the heat exchanger (E-1) the feed is heated to 277 °C. This temperature was calculated according to the energy balance that the mixture of Streams 3 and 4 must fulfill, that is, the enthalpy of the mixture must be equal to the enthalpy of Stream 5. This temperature ensures that the Zn reaches 275 °C before reaction.

The reaction step merits special attention. It should be remembered that the yield to HCOONa was fixed at 71%, and there is therefore 554 kg/h of $NaHCO_3$ remaining in the stream leaving the reactor (Stream 6). In contrast, the conversion of Zn was completed (Table 3) and it oxidizes to ZnO, specifically 2775 kg/h of ZnO were produced, as recorded in Table 3. The amount of water, as can be seen from the data gathered in Table 3, decreased slightly because 36 kg/h of hydrogen were produced. The amount of the target HCOONa obtained was about 1100 kg/h.

Previous experiments[21] proved that the conversion of $NaHCO_3$ into formate is an exothermic process, and a temperature increase (Stream 6) is therefore expected. Taking into account the values of the conversions achieved, the temperature increase was about 30 °C, which is in complete agreement with the values experimentally observed.[21]

The flow diagram present in Figure 1 shows that the products (Stream 6) are separated in a hydrocyclone (Unit S-1) into two streams: Stream 7, which contains the solids, and Stream 8, which includes the rest of the products. To calculate the amount of products in each outlet of Unit S-1, two premises were assumed: (i) the hydrocyclone can separate 100% of the ZnO and (ii) the solids leave the unit with 20% of water. In hydrocyclone technology, the split ratio refers to the ratio between the volumetric flow rate of the underflow and the volumetric flow rate of the feed. Tian et al.[53] simulated high separation efficiencies for split ratios between 0% and 10%. Therefore, a split ratio of 4% was selected in this work, which corresponds to a water content of 20% in Stream 7. The result, shown in Table 3, was a stream composed of 2775 kg/h of ZnO and 21 kg/h of $NaHCO_3$, more than 700 kg/h of H_2O, 41 kg/h of HCOONa, and a trace amount of H_2 dissolved in the liquid phase. The temperature of Streams 7 and 8 was the same as in the reactor outlet because the cooling step takes place straight after the separation of the solid ZnO.

Stream 8 needs to be cooled down to 35 °C. It is important to highlight that, in order to reduce process costs, Stream 2 and Stream 8 are energetically integrated. Therefore, Stream 8 is used as the hot stream in E-1, while Stream 2 is the cold stream. Stream 8 leaves the heat exchanger E-1 at 45 °C. To reach the target temperature of 35 °C, additional cooling is provided in the cooler (C-1), which uses cooling water at 20 °C; 80% of the water used in the cooler is recirculated. After cooling, the stream is depressurized using an isenthalpic valve, keeping the temperature practically constant.

As explained earlier, at this stage $NaHCO_3$ is considered decomposed in its equilibrium species to calculate the number of moles of CO_2 present in the mixture. Specifically, at the conditions evaluated, the molar flow rate of CO_2 is 0.016 kmol/h. In the case of water, it is important to note that one mole of water is produced per mole of CO_2 dissociated from the H_2CO_3. The mass flow rate of each substance in Stream 11 is specified in Table 3.

The last step in the process is the flash chamber (Unit S-2) separation of the liquid and gas products. CO_2, H_2, and H_2O are present in both liquid and gas phases. The gas stream (Stream 12) is formed by unreacted H_2, that is, the hydrogen produced during reaction by the reduction of the water that did not react further. Stream 12 also contains CO_2 from unreacted $NaHCO_3$ and water vapor. Stream 13 consists of a water solution containing the reaction product (HCOONa) and the unreacted $NaHCO_3$ along with its equilibrium ionic species, and dissolved gases. As one might expect, the main component of this stream is water followed by 1055 kg/h of formate.

5.3. Heat Integration. To design an environmentally friendly process and to make it more economically feasible, the heat generated when cooling the products could be used to heat the feed stream. Indeed, in the flow diagram depicted in Figure 1 there are two streams that can be integrated from an energy point of view. Stream 2 needs to be heated from 25 to 277 °C, and Stream 8 is cooled from 301 to 35 °C. From the enthalpies shown in Table 3, it can be seen that the heat

https://doi.org/10.1021/acs.iecr.1c01961
Ind. Eng. Chem. Res. 2021, 60, 14038−14050

necessary to increase the temperature of Stream 2 is 20.7 MJ/h, while the heat released by cooling down the products is 21.2 MJ/h. As is shown in Figure 5, heat integration is possible because the hot curve is over the cold curve in the temperature range considered. That is, Stream 8 can be used in the heat exchanger E-1 as the hot stream. Considering an ideal heat exchange in E-1, Stream 8 leaves this unit at 45 °C. In order to cool this stream down to 35 °C, cooler C-1 was used, employing water at 20 °C with a flow of 4000 kg/h. It should be noted that no heat losses were considered and, therefore, the heat released may be not sufficient to heat the $NaHCO_3$ solution.

5.4. Economic Analysis. The total physical costs were estimated using eq 20. First of all, the update cost of the equipment used in the process was calculated. These results are gathered in Table 4. According to eq 27, the reactor

Table 4. Process Equipment Capital Cost

equipment	cost (EUR)
reactor	450500
pump	42130
heat exchanger	56170
cooler	27590
hopper	627300
cyclone	4026
flash	4728
N_2 generator	18000
boiler	166500
PCE	1397000

volume was 21 m^3 for a 60 min residence time, and it was calculated based on water flow. The flow of Zn can be ignored. It is important to emphasize that H_2 is formed during the reaction, and the volume of the reactor may therefore be bigger. However, in this case, the Lockhart-Martinelli parameter calculated according to eq 28 was 1270 and the liquid holdup is close to 1 (see Figure 2 in the reference material[42]). Therefore, the volume of the reactor remains equal to 21 m^3.

To calculate reactor cost, the thickness of its walls was obtained using eq 29. In the reactor, the temperature reached was 301 °C and the pressure was 200 bar. The design temperature and pressure were considered as 15% higher than operating conditions. For these conditions, the reactor thickness calculated was 2.2 in. for an outside diameter of 18 in.

In the heat exchanger E-1, Stream 2 is heated from 25 to 277 °C by Stream 8, the temperature of which is lowered to 45 °C. As mentioned earlier, the target cold temperature is 35 °C, so cold water (20 °C) is used in the cooler C-1 to complete the cooling process of Stream 9. The areas of the heat exchanger and cooler (eq 25) were of 201 m^2 and 13 m^2, respectively; and their costs (eq 22) were EUR 56170 and 27590, respectively. Given that it was assumed that the hopper is filled with Zn every day, the volume needed is 9 m^3. To obtain hot water when the plant is starting up, a boiler was also designed, considering that its capacity is 25% of the mass flow. Its cost, estimated with eq 22 using the parameters gathered in Table S3,[34] was EUR 166500.

The total cost of the equipment is approximately EUR 1.4 million (Table 4). The total physical costs calculated with the Lang factors (eq 20) were nearly EUR 4.4 million (Table 5), while the fixed capital costs (eq 21) were approximately EUR 6.1 million (Table 5).

Table 5. Total Physical Capital Costs and Total Capital Costs Calculated According to Lang Factors. The Value of Lang Factor Was Taken from Sinnot[33]

f_L	concept	cost (EUR)
f_1	equipment erection	628600
f_2	piping	628600
f_3	instrumentation	209500
f_4	electrical	139700
f_5	buildings	139700
f_6	utilities	628600
f_7	storages	279400
f_8	site development	69850
f_9	auxiliary buildings	279400
	total	3003400
physical plant costs		4400400
f_{10}	design and engineering	1100000
f_{11}	contractor's fee	220000
f_{12}	contingency	440000
total		1760000
total capital costs		6160000

The variable operating costs are summarized in Table 6 and the fixed operating costs, in Table 7. It is worth mentioning

Table 6. Variable Operating Costs

variable operating costs	cost (EUR)
Raw Materials	
H_2SO_4	1196000
NaOH	2308000
Zn	1766000
Utilities	
water	62790
operation N_2 generator	4320
electricity pump	126900
electricity regeneration of ZnO	3715000
total variable operating costs	9179000

Table 7. Fixed Operating Costs

fixed operating costs	cost (EUR)
labor	567300
maintenance	308000
plant supplies	30800
supervision and management	141800
general plant costs	283700
depreciation charge	616000
taxes	61600
insurance	61600
royalties	61600
total fixed operating costs	2133000

that it was considered that the 80% of both the process and cooling water were recirculated. Therefore, the annual savings were higher than EUR 250000. The electricity needed to regenerate the ZnO by electrolysis with H_2SO_4 had a cost of EUR 3.7 million (Table 6). It should be noted that it was considered that 95% of the ZnO was recovered, making it

https://doi.org/10.1021/acs.iecr.1c01961
Ind. Eng. Chem. Res. 2021, 60, 14038−14050

necessary to buy more than 880 ton of new Zn annually, which had a cost of approximately EUR 1.8 million. The total operating costs were about EUR 11.3 million. The cost of transforming CO_2 was approximately EUR 1.6/kg of CO_2. Sodium formate can be used as a catalyst, a reducing agent, an intermediate product in the production of formic and oxalic acid, and a deicing agent, as well as in the textile and oil and gas industries, among others. A market growth rate of 4.4% is expected in the period 2020−2027, due to the increasing demand in the oil and gas, textile, and food and beverage industries and also as a deicing agent.[54] Moreover, formic acid has attracted great attention for its potential as a hydrogen storage vector, because the dehydrogenation of formic acid to generate hydrogen is a fast and easily controllable process.[55] For example, selling the sodium formate as formic acid and taking into account that formic acid with a purity of 85% can be sold for EUR 0.32/kg (although the price can fluctuate),[56] the cost of treated CO_2 drops to EUR 1.28/kg. It is also important to stress that the cost of the capture process was not considered in estimating the costs of treating the CO_2, only the cost of the NaOH used was taken into account. To make this process more economically feasible, reducing the cost of regenerating the ZnO is crucial.

6. CONCLUSIONS

In this work the technical and economic feasibility of a continuous plant for the production of sodium formate from CO_2 using Zn as the reductant was studied. It studies for the first time the main characteristics of the continuous process for CO_2 conversion in hydrothermal media. This work also demonstrates the potential for the integration of a capture and conversion system, avoiding the expensive steps associated with the separation of the captured CO_2 from the aqueous solution. Moreover, this work makes it possible to identify the strong and weak points of the process that are not evident at laboratory scale. Despite the fact that this is a first approach to the development of such a promising technology, there are still challenges to be met, from both a technical and an economic viewpoint, such as the mixture and homogenization of the solids and liquid in the reactor and the reduction of ZnO.

Results showed that yields of formic acid of 71% were achieved in a 21-m^3 reactor with a 60 min residence time at 275 °C. Heat integration was also demonstrated, the process being slightly exothermal. The total capital costs of the plant were approximately EUR 6.2 million and the cost of treated CO_2 was EUR 1.28/kg. To improve the economic feasibility of the plant, the costs of regenerating the ZnO should be reduced.

ASSOCIATED CONTENT

Supporting Information

The Supporting Information is available free of charge at https://pubs.acs.org/doi/10.1021/acs.iecr.1c01961.

Expressions for calculating C_p of Zn and ZnO at different temperatures; standard enthalpy of formation for the species involved in the production of HCOONa; parameters for calculating the physical costs of different pieces of equipment according to eq 16; substances involved in the hydrothermal conversion of $NaHCO_3$ into formate with their chemical formulas; codes BicarbonateEquilibrium, Function EqBic, PSKRtricomponent (PDF)

AUTHOR INFORMATION

Corresponding Author

Maria Dolores Bermejo − *High Pressure Process Group, Department of Chemical Engineering and Environmental Technology, Universidad de Valladolid, Valladolid 47011, Spain; BioEcoUva. Research Institute on Bioeconomy, Universidad de Valladolid, Valladolid 47011, Spain;* orcid.org/0000-0002-1693-2895; Email: mdbermejo@iq.uva.es

Authors

Laura Quintana-Gómez − *High Pressure Process Group, Department of Chemical Engineering and Environmental Technology, Universidad de Valladolid, Valladolid 47011, Spain; BioEcoUva. Research Institute on Bioeconomy, Universidad de Valladolid, Valladolid 47011, Spain*

Lidia Martínez − *High Pressure Process Group, Department of Chemical Engineering and Environmental Technology, Universidad de Valladolid, Valladolid 47011, Spain*

Daniel Román-González − *High Pressure Process Group, Department of Chemical Engineering and Environmental Technology, Universidad de Valladolid, Valladolid 47011, Spain; BioEcoUva. Research Institute on Bioeconomy, Universidad de Valladolid, Valladolid 47011, Spain*

José Juan Segovia − *BioEcoUva. Research Institute on Bioeconomy and TERMOCAL Research Group, Department of Energy and Fluid Mechanics Engineering, Universidad de Valladolid, Valladolid 47011, Spain*

Ángel Martín − *High Pressure Process Group, Department of Chemical Engineering and Environmental Technology, Universidad de Valladolid, Valladolid 47011, Spain; BioEcoUva. Research Institute on Bioeconomy, Universidad de Valladolid, Valladolid 47011, Spain*

Complete contact information is available at: https://pubs.acs.org/10.1021/acs.iecr.1c01961

Notes

The authors declare no competing financial interest.

ACKNOWLEDGMENTS

This project has been funded by the Junta de Castilla y León through project VA248P18 and JCyL and FEDER FUNDS under the BioEcoUVa Strategic Program, and by the Ministry of Science and Universities through project RTI2018-097456-B-I00. D.R.G. thanks the Spanish Ministry of Education for an FPU fellowship (FPU15/01294).

REFERENCES

(1) Sakakura, T.; Choi, J. C.; Yasuda, H. Transformation of Carbon Dioxide. *Chem. Rev.* **2007**, *107*, 2365−2387.

(2) Ma, J.; Sun, N.; Zhang, X.; Zhao, N.; Xiao, F.; Wei, W.; Sun, Y. A Short Review of Catalysis for CO_2 Conversion. *Catal. Today* **2009**, *148*, 221−231.

(3) Aresta, M.; Dibenedetto, A.; Angelini, A. The Changing Paradigm in CO_2 Utilization. *J. CO2 Util.* **2013**, *3*−*4*, 65−73.

(4) He, C.; Tian, G.; Liu, Z.; Feng, S. A Mild Hydrothermal Route to Fix Carbon Dioxide to Simple Carboxylic Acids. *Org. Lett.* **2010**, *12*, 649−651.

(5) Takahashi, H.; Kori, T.; Onoki, T.; Tohji, K.; Yamasaki, N. Hydrothermal Processing of Metal Based Compounds and Carbon Dioxide for the Synthesis of Organic Compounds. *J. Mater. Sci.* **2008**, *43*, 2487−2491.

(6) Michalkiewicz, B.; Koren, Z. C. Zeolite Membranes for Hydrogen Production from Natural Gas: State of the Art. *J. Porous Mater.* **2015**, *22*, 635−646.
(7) Jovan, D. J.; Dolanc, G. Can Green Hydrogen Production Be Economically Viable under Current Market Conditions. *Energies* **2020**, *13*, 6599.
(8) Centi, G.; Quadrelli, E. A.; Perathoner, S. Catalysis for CO_2 Conversion: A Key Technology for Rapid Introduction of Renewable Energy in the Value Chain of Chemical Industries. *Energy Environ. Sci.* **2013**, *6*, 1711−1731.
(9) Shen, Z.; Zhang, Y.; Jin, F. The Alcohol-Mediated Reduction of CO_2 and $NaHCO_3$ into Formate: A Hydrogen Transfer Reduction of $NaHCO_3$ with Glycerine under Alkaline Hydrothermal Conditions. *RSC Adv.* **2012**, *2*, 797−801.
(10) Barzagli, F.; Mani, F.; Peruzzini, M. A Comparative Study of the CO_2 Absorption in Some Solvent-Free Alkanolamines and in Aqueous Monoethanolamine (MEA). *Environ. Sci. Technol.* **2016**, *50*, 7239−7246.
(11) Kim, Y. E.; Lim, J. A.; Jeong, S. K.; Yoon, Y.Il; Bae, S. T.; Nam, S. C. Comparison of Carbon Dioxide Absorption in Aqueous MEA, DEA, TEA, and AMP Solutions. *Bull. Korean Chem. Soc.* **2013**, *34*, 783−787.
(12) Proaño, L.; Sarmiento, A. T.; Figueredo, M.; Cobo, M. Techno-Economic Evaluation of Indirect Carbonation for CO_2 Emissions Capture in Cement Industry: A System Dynamics Approach. *J. Cleaner Prod.* **2020**, *263*, 121457.
(13) Shen, Z.; Zhang, Y.; Jin, F. From $NaHCO_3$ into Formate and from Isopropanol into Acetone: Hydrogen-Transfer Reduction of $NaHCO_3$ with Isopropanol in High-Temperature Water. *Green Chem.* **2011**, *13*, 820−823.
(14) Yao, G.; Zeng, X.; Jin, Y.; Zhong, H.; Duo, J.; Jin, F. Hydrogen Production by Water Splitting with Al and In-Situ Reduction of CO_2 into Formic Acid. *Int. J. Hydrogen Energy* **2015**, *40*, 14284−14289.
(15) Huo, Z.; Hu, M.; Zeng, X.; Yun, J.; Jin, F. Catalytic Reduction of Carbon Dioxide into Methanol over Copper under Hydrothermal Conditions. *Catal. Today* **2012**, *194*, 25−29.
(16) Lyu, L.; Jin, F.; Zhong, H.; Chen, H.; Yao, G. A Novel Approach to Reduction of CO_2 into Methanol by Water Splitting with Aluminum over a Copper Catalyst. *RSC Adv.* **2015**, *5*, 31450−31453.
(17) Liu, Z.; Tian, G.; Zhu, S.; He, C.; Yue, H.; Feng, S. Ready Hydrothermal Reactions from Carbon Dioxide to Methane. *ACS Sustainable Chem. Eng.* **2013**, *1*, 313−315.
(18) Zhong, H.; Yao, G.; Cui, X.; Yan, P.; Wang, X.; Jin, F. Selective Conversion of Carbon Dioxide into Methane with a 98% Yield on an in Situ Formed Ni Nanoparticle Catalyst in Water. *Chem. Eng. J.* **2019**, *357*, 421−427.
(19) Tian, G.; He, C.; Chen, Y.; Yuan, H. M.; Liu, Z. W.; Shi, Z.; Feng, S. H. Hydrothermal Reactions from Carbon Dioxide to Phenol. *ChemSusChem* **2010**, *3*, 323−324.
(20) Duo, J.; Jin, F.; Wang, Y.; Zhong, H.; Lyu, L.; Yao, G.; Huo, Z. $NaHCO_3$-Enhanced Hydrogen Production from Water with Fe and in Situ Highly Efficient and Autocatalytic $NaHCO_3$ Reduction into Formic Acid. *Chem. Commun.* **2016**, *52*, 3316−3319.
(21) Roman-Gonzalez, D.; Moro, A.; Burgoa, F.; Pérez, E.; Nieto-Márquez, A.; Martín, Á.; Bermejo, M. D. 2Hydrothermal CO_2 Conversion Using Zinc as Reductant: Batch Reaction, Modeling and Parametric Analysisof the Process. *J. Supercrit. Fluids* **2018**, *140*, 320−328.
(22) Jin, F.; Zeng, X.; Liu, J.; Jin, Y.; Wang, L.; Zhong, H.; Yao, G.; Huo, Z. Highly Efficient and Autocatalytic H_2O Dissociation for CO_2 Reduction into Formic Acid with Zinc. *Sci. Rep.* **2015**, *4*, 1−8.
(23) Lyu, L.; Zeng, X.; Yun, J.; Wei, F.; Jin, F. No Catalyst Addition and Highly Efficient Dissociation of H_2O for the Reduction of CO_2 to Formic Acid with Mn. *Environ. Sci. Technol.* **2014**, *48*, 6003−6009.
(24) Takahashi, H.; Liu, L. H.; Yashiro, Y.; Ioku, K.; Bignall, G.; Yamasaki, N.; Kori, T. CO_2 Reduction Using Hydrothermal Method for the Selective Formation of Organic Compounds. *J. Mater. Sci.* **2006**, *41*, 1585−1589.
(25) Andérez-Fernández, M.; Pérez, E.; Martín, A.; Bermejo, M. D. Hydrothermal CO_2 Reduction Using Biomass Derivatives as Reductants. *J. Supercrit. Fluids* **2018**, *133*, 658−664.
(26) Andérez-Fernández, M.; Queiroz, J. P.; Pérez, E.; Martín, Á.; Bermejo, M. CO_2 Hydrothermal Reduction Using Glucose in a Continuous Pilot Plant. *In 7th European Meeting High Pressure Technology* **2019**, 208.
(27) Mook, W.; de Vries, J. J. *Isótopos Ambientales En El Ciclo Hidrológico. Principiosy Aplicaciones*; Guiasy manuales; Instituto Geológico y Minero de España: Madrid, 2002; Issue 1.
(28) Yoo, M.; Han, S. J.; Wee, J. H. Carbon Dioxide Capture Capacity of Sodium Hydroxide Aqueous Solution. *J. Environ. Manage.* **2013**, *114*, 512−519.
(29) Perry, R. H.; Green, D. W.; ÓHara Maloney, J. *Perry's Chemical Engineer's Handbook*; McGraw-Hill: United States of America, 1997.
(30) Spang, B. Thermodynamic and Transport Properties of Water and Steam http://www.cheresources.com/content/articles/physical-properties/thermodynamic-and-transport-properties-of-water-and-steam (accessed 2020-05-25).
(31) Thermophysical Properties of Fluid Systems. NIST Chemistry WebBook.https://webbook.nist.gov/chemistry/fluid/ (accessed 2020-10-25).
(32) Haynes, W. M.; Lide, D. R.; Bruno, T. J. *CRC Handbook of Chemistry and Physics*; CRC Press: Boca Ratón, FL, 2016.
(33) Sinnott, R. K.; Chemical Engineering Design. *Coulson & Richardson's Chemical Engineering*, 4th ed.; Elsevier Butterworth-Heinemann: Oxford, 2005; Vol. *6*
(34) Towler, G.; Sinnott, R. *Chemical Engineering Design: Principles, Practice and Economics of Plant and Process Design*; Elsevier Butterworth-Heinemann: Oxford, 2013.
(35) Yusuf, A.; Giwa, A.; Mohammed, E. O.; Mohammed, O.; Al Hajaj, A.; Abu-Zahra, M. R. M. CO_2 Utilization from Power Plant: A Comparative Techno-Economic Assessment of Soda Ash Production and Scrubbing by Monoethanolamine. *J. Cleaner Prod.* **2019**, *237*, 117760.
(36) Chemengonline. Chemical Engineering Plant Cost Index Annual Average https://www.chemengonline.com/2019-chemical-engineering-plant-cost-index-annual-average/ (accessed 2021-01-15).
(37) Coulson, J.; Richardson, J. *Chemical Engineering. Vol. 1B, Heat and Mass Transfer: Fundamentals and Applications*; Elsevier Butterworth-Heinemann: Oxford, 2018.
(38) Dabah, E.; Kannengiesser, T.; Eliezer, D.; Boellinghaus, T. In Situ Analysis of Hydrogen Behaviour in Stainless Steels by High Energy Synchrotron Radiation. *Mater. Sci. Eng., A* **2011**, *528*, 1608−1614.
(39) Asia Industrial Gases Association (AIGA). Standard for hydrogen piping systems at user locations. http://www.asiaiga.org/uploaded_docs/AIGA%20087_14_Standard%20for%20Hydrogen%20Piping%20Systems%20at%20User%20Location.pdf (accessed 2021-07-19).
(40) Dabah, E. *Hydrogen Interaction with Supermartensitic Stainless Steel Studied by Energy Dispersive X-Ray Diffraction*. Ph.D. Dissertation, Otto-Von-Guericke-Universität Magdeburg, Magdeburg, DE, 1981.
(41) MEPS. EU Stainless Steel Prices https://www.meps.co.uk/gb/en/products/europe-stainless-steel-prices (accessed 2021-01-15).
(42) Abdul-Majeed, G. H. Liquid Holdup in Horizontal Two-Phase Gas-Liquid Flow. *J. Pet. Sci. Eng.* **1996**, *15*, 271−280.
(43) Matches' 275 Equipment Cost Estimates. https://www.matche.com/equipcost/Default.html (accessed 2021-01-20).
(44) MarketsInsider. Zinc Commodity. https://markets.businessinsider.com/commodities/zinc-price (accessed 2021-01-20).
(45) Echemi. Caustic Soda Price Analysis. https://www.echemi.com/productsInformation/pd20150901041-caustic-soda-pearls.html (accessed 2021-01-20).
(46) Technologies, C. G. Nitrogen Generator Price https://nitrogen-generators.com/nitrogen-generator-price/#:~:text=Small%20flow%20nitrogen%20generators%20generally,%20generators%20are%20%24100%2C000%20and%20above (accessed 2021-03-15).

https://doi.org/10.1021/acs.iecr.1c01961
Ind. Eng. Chem. Res. 2021, 60, 14038−14050

(47) Centralair. Generadores de Nitrógeno y Oxígeno https://www.centralair.es/es/generadores-de-nitrogeno-y-oxigeno (accessed 2021-03-15).
(48) Aquavall. Tarifas del servicio de abastecimiento 2017 http://aquavall.es/wp-content/uploads/2017/06/tarifas_agua_2017.pdf (accessed 2019-10-17).
(49) Aura Energía. Tarifas Luz Industria Península https://www.aura-energia.com/tarifas-luz-industria-peninsula/ (accessed 2021-01-20).
(50) Romero Zabaleta, J. *Review of Different Technologies to Obtain Zinc from Zinc Oxide*. Dissertation, Illinois Institute of Technology, Illinois, US, 2011 https://upcommons.upc.edu/bitstream/handle/2099.1/14452/Special%20Project%20Jorge%20Romero.pdf?sequence=1 (accessed 2021-07-19).
(51) Echemi. Sulfuric Acid Price Analysis https://www.echemi.com/productsInformation/pid_Rock19440-sulfuric-acid.html (accessed 2021-03-17).
(52) Instituto Nacional de Estadística. Coste laboral anual por trabajador-año 2019 https://www.ine.es/dyngs/INEbase/es/operacion.htm?c=Estadistica_C&cid=1254736060920&menu=ultiDatos&idp=1254735976596 (accessed 2021-09-21).
(53) Tian, J.; Ni, L.; Song, T.; Shen, C.; Yao, Y.; Zhao, J. Numerical Study of Foulant-Water Separation Using Hydrocyclones Enhanced by Reflux Device: Effect of Underflow Pipe Diameter. *Sep. Purif. Technol.* **2019**, *215*, 10−24.
(54) Data Bridge Market Research1. Global Sodium Formate Market—Industry Trends and Forecast to 2027 https://www.databridgemarketresearch.com/reports/global-sodium-formate-market (accessed 2021-07-19).
(55) Santos, J. L.; Megías-Sayago, C.; Ivanova, S.; Centeno, M. Á.; Odriozola, J. A. Functionalized Biochars as Supports for Pd/C Catalysts for Efficient Hydrogen Production from Formic Acid. *Appl. Catal., B* **2021**, *282*, 119615.
(56) Echemi. Formic Acid https://www.echemi.com/produce/pr2007131046-formic-acid.html#seller_span (accessed 2021-03-18).

https://doi.org/10.1021/acs.iecr.1c01961
Ind. Eng. Chem. Res. 2021, 60, 14038−14050